Comparison of CFD and experimental performance results of a variable area ratio steam ejector

Szabolcs Varga[1], Armando C. Oliveira[1*], Xiaoli Ma[2], Siddig A. Omer[2], Wei Zhang[2] and Saffa B. Riffat[2]

[1]Faculty of Engineering, Department of Mechanical Engineering, University of Porto, Rua Roberto Frias, 4200-465 Porto, Portugal; [2]Department of Built Environment, University of Nottingham, Nottingham NG7 2RD, UK

Abstract

The advantages of numerical modelling compared with experimental studies (e.g. reduced cost, easy control of the variables, high yield etc.) are well known. Theoretical studies where experimental validation is also presented provide an important added value to numerical investigations. In the present paper, experimental and computational fluid dynamics (CFD) results for a 5-kW-rated capacity steam ejector, with a variable primary nozzle geometry, are presented and compared. The variable geometry was achieved by applying a movable spindle at the primary nozzle inlet. Relatively low operating temperatures and pressures were considered, so that the cooling system could be operated with thermal energy supplied by solar collectors (solar air-conditioning). The CFD model was based on the axi-symmetric representation of the experimental ejector, using water as a working fluid. The experimental entrainment ratio varied in the range of 0.1–0.5, depending on operating conditions and spindle tip position. It was found that the primary flow rate can be successfully adjusted by the spindle. CFD and experimental primary flow rates agreed well, with an average relative error of 8%. CFD predicted the secondary flow rate and entrainment ratio with good accuracy only in 70% of the cases.

Keywords: ejector; performance prediction; computational fluid dynamics; experimental validation

*Corresponding author: acoliv@fe.up.pt

Received 16 September 2010; revised 14 November 2010; accepted 19 November 2010

1 INTRODUCTION

The urban style of living in most warm and moderate climate countries has changed significantly over recent decades and has been accompanied by a massive increase in the use of electrical energy. Air conditioning represents a growing portion of this energy consumption. A logical solution to reduce the electricity demand would be the use of refrigeration systems that are powered by solar thermal energy. Ejector cooling seems to be an attractive technology because of its structural simplicity and low capital cost when compared with, for example, an absorption refrigerator. Although the coefficient of performance (COP) of an ejector cycle is relatively low, ejectors do not have moving parts, thus require little maintenance and have a long lifespan. Theoretical analysis of the performance characteristics of a solar-driven ejector cycle can be found in [1].

It has been realized by many researchers that it is necessary to improve the performance in order to make ejector cooling economically more attractive. A number of experimental investigations have been carried out, and some relatively recent results can be found in [2–5]. Alternatively, mathematical models can be used for analysing the performance of an ejector or the entire refrigeration cycle. A review of available models can be found in [6]. The major advantages of modelling, compared with experimental studies, are its reduced cost and the capacity of producing a large amount of performance data in a short time. Theoretical works have been reported to assess the performance of an ejector as a function of ejector geometry [7–9], working fluid [10–11] and operating conditions [12]. It should be noted that theoretical studies with experimental validation contribute to an important added value to the numerical investigations.

Reviewing the literature over the last few years, computational fluid dynamics (CFD) is becoming the usual tool to analyse and improve the performance of an ejector, by predicting both global operation and local flow structure [13]. However, there is only limited information available on comparing model results with experimental data, especially when

International Journal of Low-Carbon Technologies 2011, 6, 119–124

doi:10.1093/ijlct/ctq048 Advance Access Publication 21 December 2010

concerning real working fluids in a wide range of operating conditions. Sobieski [14] compared a 3D model with laboratory experiments, using air as a working fluid. It was concluded that model prediction was poor. In contrast, Hemidi *et al.* [13] reported that CFD predicted the global ejector performance (e.g. entrainment ratio) with good accuracy (<10%), also using air as a working fluid. In general, it was concluded that the choice of turbulence model had a high influence on the local flow features and they all showed considerable deviations from the experimental data. Rusly *et al.* [8] validated their 2D axi-symmetric CFD simulation results using R141b as a working fluid and two different turbulence models. Several ejector geometries were considered. It was found in both studies that the CFD model predicted the entrainment ratio within a 10% relative error. Good agreement between the simulated and experimental primary fluid flow rate was obtained by [15], using R123 as a working fluid. Unfortunately, only three data points were analysed. Experimental secondary fluid flow rates were less accurately predicted by CFD (25–35% error). Water was used as a working fluid in the numerical studies presented by [9]. The average simulation error for the entrainment ratio was reported to be ~5%. Larger deviations (~22%) were observed with a decreasing motive fluid temperature (pressure).

The present document discusses experimental flow measurements and numerical results for a 5-kW-rated capacity steam ejector, with variable primary nozzle geometry as a new feature. Operating conditions were considered in a range that would be suitable for an air-conditioning application, with thermal energy supplied by vacuum tube solar collectors. This implies considerably lower temperatures (pressures) on the motive fluid side than in previous studies.

2 EJECTOR DESIGN AND PERFORMANCE

The tested ejector, with a variable primary nozzle cross section, is presented in Figure 1. For a detailed description of ejector operation and their applications, the reader is referred to [16].

The performance of ejectors is often measured by the entrainment ratio (λ), defined as:

$$\lambda = \frac{\dot{m}_e}{\dot{m}_g} \tag{1}$$

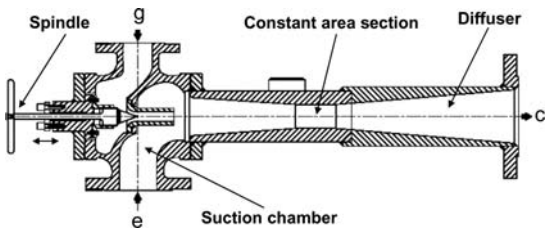

Figure 1. Drawing of a steam ejector with variable primary nozzle cross section.

where $\dot{m}_e$ and $\dot{m}_g$ are mass flow rate (in kg/s) in the evaporator and generator, respectively.

For a given cooling load, the evaporator (secondary) flow rate is approximately constant. The higher the entrainment ratio is, the lower the flow rate on the primary nozzle side is and, consequently, the lower the required heat generator input is. The entrainment ratio is related to the COP of the cooling cycle by the following expression:

$$\mathrm{COP} = \frac{Q_e}{Q_g} = \lambda \times \frac{\Delta h_e}{\Delta h_g} \tag{2}$$

where Q_e and Q_g are heat (in W) and h_e and h_g are specific enthalpy (in J/kg) in the evaporator and in the generator, respectively.

The entrainment ratio is affected by both operating conditions and geometry. For a given ejector, the performance decreases with increasing generator and with decreasing evaporator pressure/temperature [7]. The effect of the condenser condition on λ is characterized by a critical value of back pressure. Below this value, the entrainment ratio remains practically constant. This independence of λ on back pressure is probably due to the chocking of the secondary fluid [16]. Beyond the critical back pressure ($p_{c,crit}$, Pa), λ falls quickly and backflow may occur.

One of the most important geometrical factors affecting the performance of an ejector is the area ratio (r_A) between the constant area section and primary nozzle throat. In general, increasing r_A increases the entrainment ratio and decreases critical back pressure. Its optimal value is strongly affected by the applied operating conditions and can be defined as the area ratio that allows the ejector to operate in critical mode [7]. Therefore, a new feature—a spindle—was implemented, as shown in Figure 1. The function of the spindle was to provide fine tuning for the ejector operation. By changing the spindle position (SP), the area ratio (r_A) can be changed. As the spindle tip travels forward, the primary nozzle throat area decreases, and consequently r_A increases. By reducing the nozzle throat area, the primary mass flow rate also decreases. The baseline design was determined using a 1D model, similar to the one reported by [17]. The experimental test ejector was manufactured by Venturi Jet Pumps Ltd. (Stoke on Trent, UK). The most important design parameters were the cooling capacity (5 kW), steam generator (90°C), evaporator (10°C) and condenser (35°C) temperatures. Other constants such as ejector efficiencies were taken at typical values [18].

3 EXPERIMENTAL SETUP

The experimental ejector cycle with its main components is shown in Figure 2. A 24-kW electric steam generator (Fulton Boiler works, Ltd.) was used to provide high-pressure saturated steam on the primary fluid side of the ejector. The pressure of the motive fluid was adjusted according to the desired

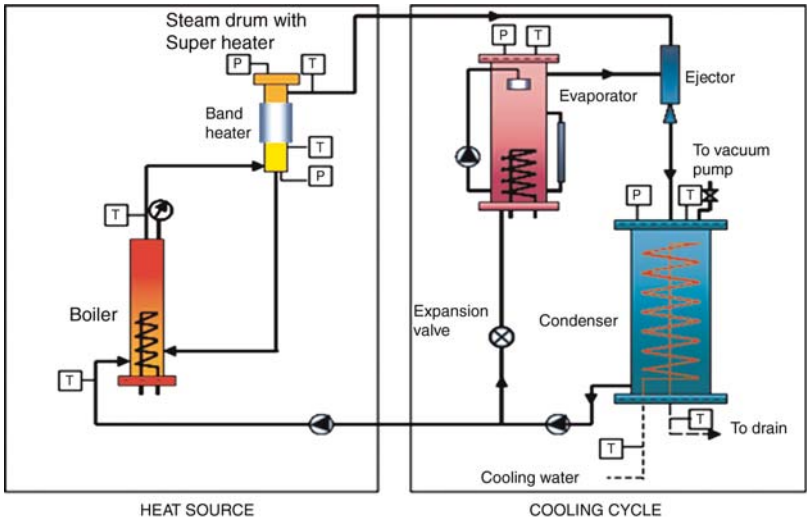

Figure 2. Schematic representation of the experimental setup.

saturation temperature. A steam drum wrapped with a 500-W electric band heater (for superheating) was used to stabilize the pressure of the primary flow from the boiler and also to increase the temperature of the primary flow by $\sim$10°C, in order to avoid unwanted condensation in the ejector. The volumetric flow rate of the motive fluid was measured before the inlet of the ejector by a high-temperature (up to 140°C) steam flow meter (FGMT212G, RM&C Roxspur Measurement & Control Ltd) with 2% full scale (FS) accuracy. The mass flow rate was calculated from the density of the steam, calculated from local temperature and pressure readings. The evaporator (see Figure 2) was a spray- and falling film-type heat exchanger. The spray was produced by a gear pump, circulating water from the evaporator bottom through a spring nozzle located at the upper part of the unit. In the present study, the cooling load was simulated by a 9-kW electric heater. The secondary flow rate was determined by measuring the water-level drop in the evaporator over time. The corresponding secondary mass flow rate can easily be calculated from the evaporator geometry and water density at T_e. The mixed water vapour leaving the ejector was condensed in a shell- and coil-type heat exchanger, using chilled water as a working fluid. Condenser pressure and temperature were controlled by adjusting the flow rate of the chilled water. Furthermore, temperature and pressure sensors were located at different points of the test rig as indicated in Figure 2. Type T thermocouples ($\pm$0.25°C) were applied for the temperature measurements, and the static pressure was monitored using Druck PTX 1400 transducers ($\pm$0.25% FS). Experimental data were recorded on the PC connected to a Datataker DT 500 (Grant Instruments Ltd.) data logger.

Experiments were carried out under steady-state operating conditions. After starting up, the system was left to reach equilibrium with respect to the monitored temperatures at all measurement points. As it was mentioned before, test conditions were selected in a range that would be suitable to use vacuum-type solar collectors as heat source. Generator and condenser temperatures were kept in the range of 85–95°C and 25–37°C, respectively. Evaporator temperature was maintained at $\sim$10°C.

4 CFD MODEL

Fluid flow in the ejector is typically compressible and turbulent. In the present case, the only reasonable simplifying assumption that could be made was axi-symmetry [9]. The functional relationship between the three major unknown variables—temperature (T), pressure (p) and velocity vector ($\mathbf{v}$)—describing compressible flow of an isotropic Newtonian fluids is given by the conservation of energy, momentum and continuity equations, in the form of a set of partial differential equations (PDEs). The turbulent behaviour was treated using the Reynolds averaging principle (RANS). The realizable version of the k-ϵ turbulence model was chosen in this work. For more details of the numerical model and the computational domain, the reader is referred to [7]. In order to solve the fluid flow inside the ejector, proper boundary conditions (BCs) must be applied. Pressure BCs were applied at the inlets, according to saturation conditions depending on the temperatures in the generator and evaporator. At the outlet, a pressure BC was chosen according to the condenser pressure of the ejector cooling cycle. This is a reasonable choice when it is assumed that the transport losses between the ejector outlet and the condenser are negligible. Heat transfer through the walls was neglected (zero heat flux). In this work, a commercial package—FLUENT 6.3—was used to simulate fluid flow in the ejector. In FLUENT, the space domain is subdivided into a number of small control volumes called finite volumes. For each finite volume, each PDE is transformed into a set of algebraic equations and then solved using numerical techniques. The unknown quantities were calculated for each cell centre using a combination of a segregated and a coupled algorithm.

In order to optimize the CFD model, several mesh densities were examined, from the finer to the coarser. The final structured mesh consisted of $\sim 6 \times 10^4$ quadrangular cells.

5 RESULTS AND DISCUSSION

The effect of the spindle tip position on the primary flow rate was tested for a set of operating conditions. SP was varied from zero (completely closed) to 30 mm (fully open) and the secondary flow rate was kept at zero. Experimental results obtained for different generator pressures are summarized in Table 1. It can be seen that the primary flow rate varied in the range of 2.0×10^{-3} to 6.5×10^{-3} kg/s. In general, it increased with increasing the free cross section in the primary nozzle. However, it showed a significant variation for constant SP depending on steam generator pressure. CFD results with the corresponding relative error (e_r) between simulation and experiments are also indicated in Table 1. It can be seen that e_r showed a maximum as high as $\sim$15% for SP = 15 mm; however, the average error was as low as 2.8%. Considering the absolute value of the relative error, it had an average value of 7.7%, which is comparable with previously published data. It can be concluded that, in spite of some deviation, CFD could generally predict the primary flow rate with an acceptable accuracy.

Results obtained for the secondary flow rate are summarized in Table 2. It can be seen from the table that experimentally determined secondary flow rates varied considerably depending on operating conditions (0.65–1.9 g/s). Comparing the results obtained by the CFD model to the experimental measurements, it was found that in $\sim$70% of the cases, the predicted flow rates were in good agreement with the observed data (error $<$20%), while for some other cases the difference was very large ($\geq$30%). These results are also visualized in Figure 3. It is clear from the figure that in those cases where CFD failed to predict $\bar{m}_e$, simulation resulted in significantly higher values. The average error was found to be $\sim$18%, which is smaller than the error previously reported by [15] using R123 as a working fluid. The relatively large difference between CFD and experimental data could be explained by the fact that CFD was carried out in the double-chocking operating range, where the performance of an ejector is independent from downstream pressure, while during the experiments the ejector might have been operated in single chocking mode. This hypothesis, however, was not experimentally confirmed. Another reason for the poor CFD prediction could be related to the uncertainty in the static pressure measurement in the evaporator. In the present work, ejector operation was tested for relatively low evaporator pressures ($\sim$1 kPa). The typical error of the pressure sensors was in the range of 150 Pa. Simulation results indicated that a change in the upstream pressure on the evaporator side resulted in an $\sim$20% reduction in the secondary fluid flow rate.

The entrainment ratio resulting from experimental flow rate measurements and CFD simulations was also compared. These results are presented in Figure 4. Experimentally determined λ varied in the range of 0.1–0.5, depending on operating conditions and SP. Such as for the secondary fluid flow rate, simulations resulted in an acceptable prediction for approximately two-third of the cases, while for the other cases the CFD model significantly over-predicted λ, probably due to the same reasoning. The average error was $\sim$20% mostly due to the increased error in the secondary flow rate. Direct comparison of the present CFD model performance to previously published data is difficult, due to the difference in operating conditions, ejector design and working fluid applied. Pianthong

Table 1. Primary flow rate as a function of SP and generator pressure.

SP, mm	p_g, kPa	$\dot{m}_{g,exp}$, g/s	$\dot{m}_{g,sim}$, g/s	e_r, %
2	61.3	2.0	2.0	−1.8
5	117.9	3.6	3.9	−6.5
8	56.4	2.5	2.6	−4.9
10	103.7	5.2	4.8	8.3
10	67.1	2.9	3.1	−7.1
10	93.9	4.8	4.3	10.6
14	52.8	3.1	3.1	2.2
15	90.5	5.8	5.2	9.7
15	61.0	3.1	3.6	−14.6
20	52.6	3.1	3.6	−13.8
20	85.4	6.4	5.7	10.8
20	79.1	5.9	5.3	10.6
20	76.9	5.4	5.2	4.4
21	48.5	3.3	3.3	−0.7
21	68.8	5.2	4.6	11.0
21	56.9	4.3	3.8	11.0
21	58.7	4.4	4.0	9.9
21	56.3	4.2	3.8	8.3
21	54.7	3.9	3.7	4.2
25	71.7	5.9	5.4	7.8
25	77.2	6.5	5.8	10.7
25	55.8	4.3	4.3	0.7
30	63.4	5.8	5.2	10.1
30	42.5	3.1	3.5	−13.1
30	53.8	4.5	4.4	2.4
30	49.8	4.3	4.1	3.6

Table 2. Experimental and simulated secondary flow rates for different operating conditions.

SP, mm	p_e, Pa	T_e, °C	$\dot{m}_{e,exp}$, g/s	$\dot{m}_{e,sim}$g/s	e_r, %
2	987	10.2	0.65	1.6	59.9
8	978	10.5	0.84	1.6	47.7
14	1012	9.5	1.0	1.0	3.2
21	1113	10.9	0.96	1.6	40.6
21	1119	11.1	1.2	1.7	29.1
21	1004	10.9	1.7	1.6	−8.3
21	1004	10.5	1.3	1.5	15.1
21	1008	10.2	1.2	1.5	22.1
21	963	10.5	1.4	1.3	−12
21	1019	10.5	1.5	1.6	6.4
21	865	7.8	1.0	1.2	13.1
21	1189	12.8	1.9	1.9	−1.2
25	849	9.0	1.2	1.2	−3.0
30	886	10.8	1.4	1.3	−1.3

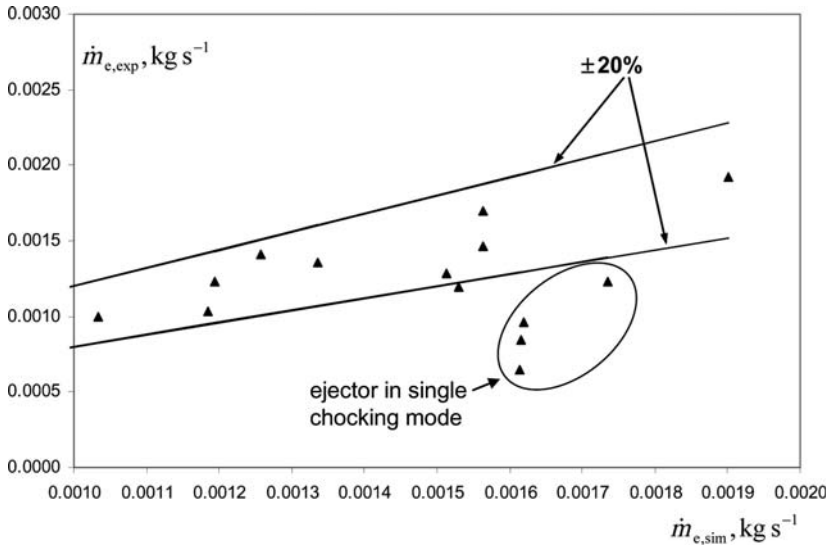

Figure 3. Comparison of experimental and simulated secondary flow rates.

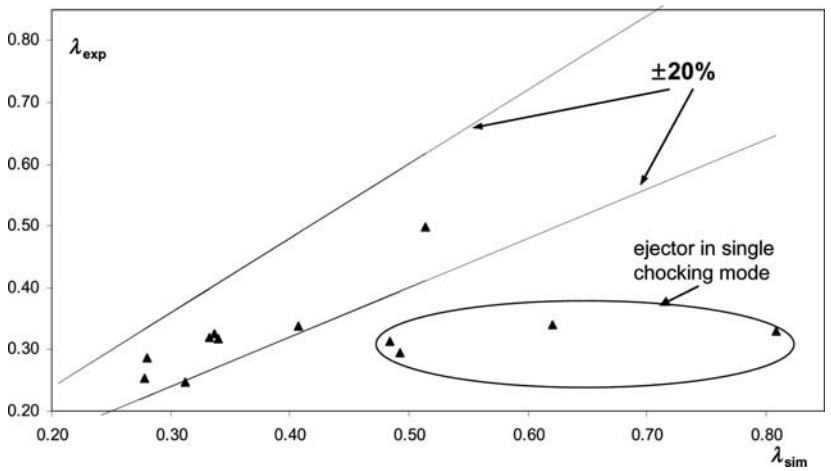

Figure 4. Comparison of experimental and simulated entrainment ratios.

et al. [9] reported an excellent 5% average simulation error for the entrainment ratio, whereas Sriveerakul *et al.* [19] obtained CFD predictions within 15% of the measurements using water as operating fluid. In both cases, however, a smaller ejector was simulated and the applied operating conditions corresponded to a higher upstream temperature/pressure. For example, Pianthong *et al.* [9] considered generator temperatures in the range of 120–140°C. Analysing the graphical data presented, it was found that the simulation error increased with decreasing T_g, and a deviation of ~22% was estimated for 120°C.

6 CONCLUSIONS

Experimental and numerical results for the performance of a 5-kW cooling capacity steam ejector, with variable primary nozzle geometry, were presented and compared. Operating conditions were considered in a range that would be suitable for an air-conditioning application, with thermal energy supplied by vacuum tube solar collectors. It was found that CFD predicted the motive fluid flow rate for all operating conditions and SPs with good accuracy. The average relative error equals 7.7%.

The CFD-simulated secondary flow rate and entrainment ratio resulted in an acceptable accuracy for only 70% of the cases, while significant over prediction of the CFD model was observed for the rest of the data points. This over prediction could be explained by the fact that simulations were carried out under double chocking conditions, while the experimental measurements could have been performed under single chocking conditions. However, this theory has not been experimentally confirmed. It was also pointed out that an accurate measurement of the evaporator pressure is important, because a small uncertainty on the low pressure side of the ejector may result in significant differences in the simulated ejector performance. A small adjustment in the evaporator pressure

(<0.2 kPa) resulted in very good agreement between the simulated and experimental entrainment ratio. Therefore, a more complete sensitivity analysis should be carried out in order to analyse the influence of uncertainty in experimentally measured variables (e.g. temperatures, pressures and flow rates) on the validation of steam ejector CFD models, under design and off-design operating conditions.

ACKNOWLEDGEMENTS

This work was developed within the framework of the Mediterranean-Aircond Project, which was funded by the Commission of the European Union (DG Research), through the Energy research programme (FP6): contract INCO-CT2006-032227. The authors would also like to acknowledge other project partners, namely the University of Nottingham (UK) and Venturi Jet Pumps (UK).

REFERENCES

[1] Varga Sz, Oliveira AC, Diaconu B. Analysis of a solar-assisted ejector cooling system for air conditioning. *Int J Low Carbon Technologies* 2009;**4**:2–8.

[2] Eames IW, Ablwaifa AE, Petrenko V. Results of an experimental study of an advanced jet-pump refrigerator operating with R245fa. *Appl Therm Eng* 2007;**27**:2833–40.

[3] Yapici R, Ersoy HK, Aktoprakoğlu A, Halkaci HS, Yiğit O. Experimental determination of the optimum performance of ejector refrigeration system depending on ejector area ratio. *Int J Refrigeration* 2008;**31**:1183–189.

[4] Sankarlal T, Mani A. Experimental investigations on ejector refrigeration system with ammonia. *Renew Energy* 2007;**32**:1403–413.

[5] Godefroy J, Boukhanouf R, Riffat S. Design, testing and mathematical modelling of a small-scale CHP and cooling system (small CHP-ejector trigeneration). *Appl Therm Eng* 2007;**27**:68–77.

[6] He S, Li Y, Wang RZ. Progress of mathematical modeling on ejectors. *Renew Sust Energy Rev* 2009;**13**:1760–780.

[7] Varga Sz, Oliveira AC, Diaconu B. Influence of geometrical factors on steam ejector performance – a numerical assessment. *Int J Refrigeration* 2009;**32**:1694–701.

[8] Rusly E, Aye L, Charters WWS, Ooi A. CFD analysis of ejector in a combined ejector cooling system. *Int J Refrigeration* 2005;**28**:1092–101.

[9] Pianthong K, Sheehanam W, Behnia M, Sriveerakul T, Aphornratana S. Investigation and improvement of ejector refrigeration system using computational fluid dynamics technique. *Energy Convers Manage* 2007;**48**:2556–564.

[10] Sun Da-W. Comparative study of the performance of an ejector refrigeration cycle operating with various refrigerants. *Energy Convers Manage* 1999;**40**:873–84.

[11] Cizungu K, Mani A, Groll M. Performance comparison of vapour jet refrigeration system with environment friendly working fluids. *Appl Therm Eng* 2001;**21**:585–98.

[12] Boumaraf L, Lallemand A. Modeling of an ejector refrigerating system operating in dimensioning and off-dimensioning conditions with the working fluids R142b and R600a. *Appl Thermal Eng* 2009;**29**:265–74.

[13] Hemidi A, Henry F, Leclair S, Seynhaeve J-M, Bartosiewicz Y. CFD analysis of a supersonic air ejector. Part II: Relation between global operation and local flow features. *Appl Thermal Eng* 2009;**29**:2990–998.

[14] Sobieski W. Performance of an air-air ejector: an attempt at numerical modelling. *Task Q* 2003;**7**:449–57.

[15] Smierciew K, Butrymowicz D, Karwacki J, Trela M. Modelling of ejection cycle for solar air-conditioning. In: *International Seminar on Ejector/Jetpump Technology and Application*, Louvain-la-Neuve, Belgium, 2009, Sept. 7–9, paper N° 25.

[16] Chunnanond K, Aphornratana S. Ejectors: application in refrigeration technology. *Renew Sust Energy Rev* 2004;**8**:129–55.

[17] Huang BJ, Chang JM, Wang CP, Petrenko VA. A 1-D analysis of ejector performance. *Int J Refrigeration* 1999;**22**:354–64.

[18] Varga Sz, Oliveira AC, Diaconu B. Numerical assessment of steam ejector efficiencies using CFD. *Int J Refrigeration* 2009;**32**:1203–211.

[19] Sriveerakul T, Aphornratana S, Chunnanond K. Performance prediction of steam ejector using computational fluid dynamics: Part 1. Validation of the CFD results. *Int J Thermal Sci* 2007;**46**:812–22.